Solution Equilibrium Studies on Anticancer Ruthenium(II)–η^6-*p*-cymene Complexes of 3-Hydroxy-2(1*H*)-pyridones

Éva A. Enyedy[a,*], Gabriella M. Bognár[a], Tamás Kiss[a,b], Muhammad Hanif[c], Christian G. Hartinger[c,d,*]

[a] Department of Inorganic and Analytical Chemistry, University of Szeged, Dóm tér 7. H-6720 Szeged, Hungary

[b] Bioinorganic Chemistry Research Group of the Hungarian Academy of Sciences, University of Szeged, Dóm tér 7. H-6720 Szeged, Hungary

[c] Institute of Inorganic Chemistry, University of Vienna, Waehringer Str. 42, A-1090 Vienna, Austria

[d] The University of Auckland, School of Chemical Sciences, Private Bag 92019, Auckland 1142, New Zealand

* Corresponding authors: Fax: +36 62 420505; and +64 9 373 7599 ext 83220

E-mail addresses: enyedy@chem.u-szeged.hu (É. A. Enyedy) and c.hartinger@auckland.ac.nz (C. G. Hartinger)

ABSTRACT

$Ru^{II}(\eta^6$-p-cymene) complexes of two bidentate (O,O) alkoxycarbonylmethyl-3-hydroxy-2(1H)-pyridone ligands exhibit *in vitro* antitumor activity. We determined their stoichiometry and stability in aqueous solution by pH-potentiometry, ^{1}H NMR spectroscopy and UV-Vis spectrophotometry and also characterized the proton dissociation processes of the ligands. Formation of mono-ligand complexes with moderate stability was found to predominate in the physiological pH range. Moreover, the chlorido/aqua co-ligand exchange processes of the $[Ru^{II}(\eta^6$-p-cymene)(L)(H$_2$O)]$^+$ species were also monitored and 55–65% of the aqua ligand was found to be replaced by chloride in 0.2 M KCl containing aqueous solutions. Under basic conditions, the complexes decompose to dinuclear tri-hydroxido-bridged $[Ru_2(\eta^6$-p-cymene)$_2$(OH)$_3$]$^+$ and metal-free ligand and also a hydroxido species $[Ru^{II}(\eta^6$-p-cymene)(L)(OH)] was found. Furthermore, the ligands contain an ester functional group, which may hydrolyze at basic pH, which is however negligible at acidic or neutral pH.

1. Introduction

Anticancer metallodrug research started with the discovery of cisplatin and its introduction to clinical practice almost four decades ago [1,2]. The main goal of the development of novel anticancer metal-based compounds is to increase their selectivity and therapeutic index and thereby overcome the adverse effects and resistance phenomena, which are a major limitation for the curative treatment of cancer. Ruthenium compounds are currently considered as the most promising candidates for the next generation of antitumor metal complexes [2−4]. Two representatives of this class of compounds have entered clinical trials so far, *i.e.*, imidazolium trans-[tetrachlorido(dimethylsulfoxide)(1*H*-imidazole)ruthenate(III)] (NAMI-A) [5,6] and indazolium trans-[tetrachloridobis(1*H*-indazole)ruthenate(III)] (KP1019) [7,8]. The reduction of Ru^{III} complexes to Ru^{II} in the more reductive tumor environment as compared to normal tissue is an important step of activation. In addition to Ru^{III} coordination compounds, organometallic Ru^{II} complexes mainly with piano stool structure were developed and tested *in vitro* and *in vivo*. Among the Ru^{II}(arene) complexes a large number of $[Ru^{II}(\eta^6\text{-}p\text{-}$ cymene)(XY)Cl]-type compounds were prepared, where XY is an (*O,O*), (*O,S*), (*O,N*), (*N,N*) or (*N,S*) bidentate ligand [9−16]. The replacement of chlorido by aqua ligands can take place in aqueous solution, which is considered an essential step of activation [17−20]. However, the ultimate target of these organometallic Ru^{II}(arene) complexes is still not clear [21,22]. As other anticancer metallodrugs, they can be regarded as prodrugs and it is a prerequisite to follow their speciation in biological fluids for a better understanding of the pharmacokinetic properties and the mechanism of action. Aqueous solution equilibrium studies are a first approach to characterize possible dissociation reactions of such metal complexes in solution at low concentration. The displacement of original ligands by endogenous biomolecules strongly depends on the thermodynamic stability and kinetic inertness/lability. However, little is known about the stability of Ru^{II}(arene) complexes. Buglyó and co-workers determined stability data for $Ru^{II}(\eta^6\text{-}p\text{-}$cymene) complexes with bidentate (*O,O*) ligands [23,24], and also the pK_a values of the coordinated water molecule in $[Ru^{II}(\eta^6\text{-}p\text{-}$cymene)(XY)(H$_2$O)] species were reported [9,18,24,25]. Complexes bearing (*O,O*) bound hydroxypyrones show only moderate cytotoxicity and much lower stability as compared to (*O,N*) or (*O,S*) type complexes [26,27]. Switching from hydroxypyrones (such as the well-known maltol) to hydroxypyridones allows tuning the chelating ability and drug-like parameters, such as lipophilicity [18]. The Ru complex $[Ru^{II}(\eta^6\text{-}p\text{-}$cymene)(**EHP**)Cl] {**EHP** = *N-*

[(ethoxycarbonyl)methyl]-3-hydroxy-2-(1H)-pyridone} was previously prepared and evaluated as an anticancer agent in CH1 adenocarcinoma human cells of the ovary, showing moderate cytotoxicity (IC$_{50}$ 240 μM) [18].

In this work, the behavior of Ru^{II}(η^6-p-cymene) complexes of the alkoxycarbonylmethyl-3-hydroxy-2(1H)-pyridone ligands, *i.e.*, **EHP** and *N*-[(ethoxycarbonyl)methyl]-3-hydroxy-4-methyl-2-(1H)-pyridone (**EHMP**) (Chart 1) in aqueous solution was studied by pH-potentiometry, ^{1}H NMR spectroscopy and UV-Vis spectrophotometry in order to determine the stoichiometry and stability of the complexes as well as the proton dissociation processes of the ligands.

Chart 1

2. Experimental

2.1. Chemicals

The ligands **EHP** and **EHMP** were prepared as described previously [18]. The purity and hydrolytic stability of the ligands was checked and the exact concentrations of the stock solutions were determined by the Gran method [28]. [Ru^{II}(η^6-p-cymene)Cl$_2$]$_2$ was synthesized and purified according to a literature procedure [29]. A stock solution of [Ru^{II}(η^6-p-cymene)] was obtained by dissolving a known amount of [Ru^{II}(η^6-p-cymene)Cl$_2$]$_2$ in water and the exact concentration was determined with pH-potentiometric titrations employing literature data for [Ru^{II}(η^6-p-cymene)]–hydroxido complexes [23].

2.2. pH-potentiometric measurements

The pH-potentiometric measurements for determination of the protonation constants of the ligands and the overall stability constants of the metal complexes were carried out at 25.0 ± 0.1 °C in water and at an ionic strength of 0.20 M (KCl, Sigma-Aldrich) in order to keep the activity coefficients constant. The titrations were performed with carbonate-free KOH solution of known concentration (0.20 M). Both the base and the HCl used were Sigma-Aldrich products and their concentrations were determined by pH-potentiometric titrations.

An Orion 710A pH-meter equipped with a Metrohm combined electrode (type 6.0234.100) and a Metrohm 665 Dosimat burette were used for the pH-potentiometric measurements. The electrode system was calibrated to the pH = −log[H$^+$] scale by means of blank titrations (strong acid *vs.* strong base: HCl *vs.* KOH), as suggested by Irving *et al.* [30]. The average water ionization constant, pK_w, was determined as 13.76 ± 0.01 at 25.0 °C, I = 0.20 M (KCl), which corresponds well to the literature [31]. The reproducibility of the titration points included in the calculations was within 0.005 pH. The pH-potentiometric titrations were performed in the pH range 2.0−11.5. The initial volume of the samples was 10.0 mL. The ligand concentration was 2×10^{-3} M and metal ion-to-ligand ratios of 1:1 to 1:4 were used. The accepted fitting of the titration curves was always less than 10 μL. Samples were degassed by bubbling purified argon through them for *ca.* 10 min prior to the measurements and it was also passed over the solutions during the titrations.

For testing the hydrolytic stability of the ligands, stock solutions were prepared at various pH values (pH 1.83, 7.61 and 11.11) and titrations were performed at pH 1.83 after 0.5, 47 and 191 h, at pH 7.61 after 1, 48 and 120 h and at pH 11.11 after 0.17, 0.33, 1.42, 1.62, 2.7, 4, 24 and 188 h.

The protonation constants of the ligands were determined with the computer program HYPERQUAD [32]; PSEQUAD [33] was utilized to establish the stoichiometry of the complexes and to calculate the stability constants. $\beta\,(M_pL_qH_r)$ is defined for the general equilibrium $p\mathrm{M} + q\mathrm{L} + r\mathrm{H} \rightleftharpoons M_pL_qH_r$ as $\beta(M_pL_qH_r) = [M_pL_qH_r]/[M]^p[L]^q[H]^r$ where M denotes a metal ion and L the completely deprotonated ligand. Literature $\log\beta$ values of the [Ru^{II}(η^6-*p*-cymene)(hydroxido)] complexes were used [23] and compared to data collected in the course of the experiments described herein. In all calculations exclusively titration data were used from experiments in which no precipitate was visible in the reaction mixture.

2.3. UV–Vis spectrophotometric and ^{1}H NMR measurements

A Hewlett Packard 8452A diode array spectrophotometer was used to record the UV-Vis spectra in the interval 200–800 nm. The path length was 1 cm. Protonation and stability constants and the individual spectra of the species were calculated with the computer program PSEQUAD [33]. The spectrophotometric titrations were performed on samples of the ligands alone or with [Ru^{II}(η^6-*p*-cymene)] over the pH range 2.0–11.5 at an ionic strength of 0.20 M

(KCl) and at 25.0 ± 0.2 °C. The concentration of ligands was set constant at 1×10^{-4} M and the metal-to-ligand ratios were 1:1 and 1:2.

^{1}H NMR studies were carried out on a Bruker Ultrashield 500 Plus instrument. 4,4-Dimethyl-4-silapentane-1-sulfonic acid was used as an NMR standard. The ligands were dissolved in a 10% (v/v) D_2O/H_2O mixture to yield a concentration of 2−4 mM and were titrated at 25 °C, at $I = 0.20$ M (KCl) in absence or presence of [Ru^{II}(η^6-p-cymene)] at 1:1 and 1:2 metal-to-ligand ratios. ^{1}H NMR spectra were recorded to study the H_2O/Cl^- exchange processes in the [Ru^{II}(η^6-p-cymene)(L)] complexes at pH 5.8 and 7.4 in dependence of the Cl^- concentration (4−500 mM).

2.4. Determination of the distribution coefficient (logD$_{7.4}$) of EHP and EHMP

Log$D_{7.4}$ values of **EHP** and **EHMP** were determined by the traditional shake flask method [34] in *n*-octanol/HEPES-buffered aqueous solution at pH 7.4 (4-(2-hydroxyethyl)-1-piperazineethanesulfonic acid, HEPES) at 25.0 ± 0.2 °C. Two parallel experiments were performed for each sample. The ligands were dissolved at 0.10 mM in *n*-octanol pre-saturated aqueous solution of the buffer (10 mM) at constant ionic strength (0.20 M KCl). The aqueous solutions and *n*-octanol (1:1) were gently mixed with 360° vertical rotation for 2 h to avoid emulsion formation, and the mixtures were centrifuged at 5000 rpm for 3 min with a HeroLab centrifuge. After separation of the phases, UV spectra of the ligands in the aqueous phase were compared with those of the original aqueous solutions in the range 250–400 nm and log$D_{7.4}$ values were calculated using equation 1.

$$\log D_{7.4} = \log \left(\frac{Absorbance_{original\ solution}}{Absorbance_{aqueous\ phase}} - 1 \right) \tag{1}$$

The absorbance was obtained at the region of λ_{max} (~300 nm) ± 10 nm. The partition coefficients (log$P$) of **EHP** and **EHMP** were calculated using equation 2.

$$\log P = \log \left(D \times (1 + (K_a / [H^+])) \right) \tag{2}$$

3. Results and discussion

3.1. Proton dissociation processes and lipophilicity of the ligands

The proton dissociation processes of the ligands **EHP** and **EHMP** (Chart 1) in water were followed by pH-potentiometry, UV spectrophotometry and ^{1}H NMR titrations. The ligands contain ester functional groups and thus may undergo hydrolysis under acidic and basic conditions. Therefore, before studying the solution equilibria of the Ru complexes, a careful investigation of the hydrolytic stability of **EHP** and **EHMP** had to be performed. Stock solutions containing either ligand were prepared at pH 1.83, 7.61 and 11.11 and aliquots were titrated with the strong base KOH within a time frame of up to 191 h (Fig. S1). The formation of the carboxylic acid moiety by hydrolysis of the ester bond would result in extra base consumption and a shift of the equivalent point, which was only observed at pH 11.11. Within 3 h *ca.* 45% of the ester had hydrolyzed, and remained constant during the rest of the experiment (Fig, S1.d). The hydrolytic stability of the ligands was also monitored by a second titration following re-acidification of the initially titrated aliquots of the acidic stock solution with the base. Overlapping consecutive titration curves were observed when the first titration was stopped at a maximum of pH ~10.4, demonstrating that no measurable ester hydrolysis of **EHP** and **EHMP** takes place between pH 2 and 10.4. In addition, the hydrolysis of **EHP** was monitored at pH 7.4 by ^{1}H NMR spectroscopy (Fig. S2), which revealed that no measurable hydrolysis takes place at this pH value within 168 h. Based on these preliminary results, the proton dissociation constants (pK_a) of the ligands were calculated from data collected in the pH range 2.0−10.4. The pK_a values determined by the pH-potentiometric, UV and ^{1}H NMR titrations are collected in Table 1 and are in a fairly good agreement. The proton dissociation constants can be attributed to the deprotonation of the hydroxyl functional group. The pK_a of **EHP** was found to be somewhat lower than that of the structurally related 3-hydroxy-1-methylpyrid-2(1*H*)-one (MH2P, pK_a = 8.89 [35]) due to the electron-withdrawing effect of the ester moiety. The presence of the neighboring electron-donating methyl group adjacent to the hydroxyl in **EHMP** results in higher basicity compared to **EHP** and MH2P. The deprotonation of **EHP** and **EHMP** is accompanied by characteristic changes of the ligand bands in the UV spectra (for **EHP** see Fig. 1). The development of new strong bands at a higher λ_{max} value was observed for both ligands due to deprotonation which results in more extended conjugated π electron systems. The individual UV spectra of the ligand species (HL

and L$^-$) were also calculated on basis of deconvolution of the pH-dependent spectra (Fig. S3 and Table 1). The constant location of the isosbestic points in the spectra of the ligands (see Fig. 1 for **EHP**) also indicates that the ester hydrolysis is negligible in the pH range studied (pH 2.0–10.4).

Table 1

Fig. 1.

^{1}H NMR spectroscopic titrations of the ligands gave very similar results (see Fig. 2 for **EHP**, Fig. S4 for **EHMP**). The chemical shifts (δ) of the aromatic CH protons are sensitive to the protonation state of the ligands, and upfield shifts of these protons of **EHP** by increasing pH are as shown in Fig. 3. Based on these changes, the pK_a values and chemical shifts of the individual ligand species (HL; L$^-$) were calculated (Table 1). Above pH 10, signals were assigned to the hydrolysis products, *i.e.* the corresponding 3-hydroxy-2-oxopyridine-1(2H)-carboxylate and ethanol (Fig. 2).

Figs. 2, 3.

Furthermore, **EHP** and **EHMP** were also characterized with regard to their lipophilicity and distribution coefficients at physiological pH (log$D_{7.4}$), as determined via *n*-octanol/water partitioning. The partition coefficients (log$P$) of the neutral, non-ionized species were calculated from the log$D_{7.4}$ values using the proton dissociation constants (Table 1). **EHMP** exhibits a more lipophilic character than **EHP** due to the additional methyl group.

3.2. Solution equilibria of [Ru^{II}(η^6-p-cymene)] complexes of *EHP* and *EHMP*

The complex formation processes of the ligands with [Ru^{II}(η^6-*p*-cymene)(H$_2$O)$_3$]$^{2+}$ were studied by pH-potentiometry, UV-Vis spectrophotometry and ^{1}H NMR spectroscopy in aqueous solution. The stability constants of the minor and major dinuclear hydrolysis products [Ru$_2$(η^6-*p*-cymene)$_2$(OH)$_2$]$^{2+}$ and [Ru$_2$(η^6-*p*-cymene)$_2$(OH)$_3$]$^+$, respectively, were determined by pH-potentiometry in the presence of 0.2 M KCl (Table 2) and were found to be in good agreement with data obtained by Buglyó and colleagues [23]. The chloride ion is considered as a non-innocent ligand for Ru^{II} [19,20,36], and thus these stability data are regarded as

conditional stability constants and are valid under the given conditions (0.2 M KCl, $T = 25$ °C). The aqueous solution behavior of [Ru^{II}(η^6-p-cymene)] can be described well with the formation of the above mentioned three kinds of species at 0.2 M KCl ionic strength [23,24]. However various chlorido, hydroxido and mixed chlorido-hydroxido complexes are present at acidic pH, rather than [Ru^{II}(η^6-p-cymene)(H$_2$O)$_3$]$^{2+}$ and [Ru$_2$(η^6-p-cymene)$_2$(OH)$_2$]$^{2+}$ [36]. Above pH ~6.5 the dinuclear complex [Ru$_2$(η^6-p-cymene)$_2$(μ^2-OH)$_3$]$^+$ predominates [23,36]. It was also found that the hydrolytic equilibria are reached quickly so that pH-potentiometric titrations can be employed to follow the process.

The formation of the Ru^{II}(η^6-p-cymene) complexes with the ligands **EHP** and **EHMP** starts in the acidic pH range and the exclusive formation of mononuclear species with 1:1 metal-to-ligand ratio was identified. Stability constants of the complexes [Ru^{II}(η^6-p-cymene)(L)] were determined by pH-potentiometry and UV-Vis spectrophotometry monitoring complex formation via the changes of the charge transfer (CT) bands and they are in good agreement with each other (Table 2). In these complexes the bidentate (O,O) coordination mode of the ligands is the most feasible in solution, similarly to other hydroxypyridone compounds [37] as demonstrated by single-crystal X-ray diffraction studies [18]. Due to the slow ligand exchange processes observed in the ^{1}H NMR spectra of the complexes with respect to the NMR time scale, the chemical shifts of the protons of the free and bound ligand and the Ru^{II}(η^6-p-cymene) moiety are clearly distinguishable (Figs. 4, 5, Fig. S5).

Figs. 4, 5.

The integrals of the pH-dependent proton peaks of the non-bound ligand and Ru^{II}(η^6-p-cymene) moiety and the peaks of the metal complexes are proportional to the molar fractions of the species (Fig. 6). The molar fractions of the bound and free metal ions were also calculated on basis of the determined stability constants. Very good correlation between the pH-potentiometric and ^{1}H NMR spectroscopic data were observed at pH < *ca.* 6. Up to this pH the formation of [Ru^{II}(η^6-p-cymene)(L)] reaches a maximum and good quality ^{1}H NMR data was accessible (Fig. 4, Tables S1, S2). The aromatic ring protons of the ligands and all the protons of the Ru^{II}(η^6-p-cymene) moiety show significant electronic shielding effects as compared with the HL ligand forms and ligand-free organometallic arene moiety.

Fig. 6.

The *mono*-ligand [Ru^{II}(η^6-*p*-cymene)(L)] species, in which L is a bidentate ligand, often bear a chlorido leaving group, as also shown in the solid state by X-ray diffraction analysis [9,18,38,39]. These compounds can undergo aquation of the chlorido ligand in aqueous solution. This exchange process usually takes place fast and is considered to be an important step for the biological activation of the metal complex [17−20]. The extent of the aquation strongly depends on the type of the bidentate ligand and the actual chloride concentration [17−20,36]. Therefore, the [Ru^{II}(η^6-*p*-cymene)(L)(H$_2$O)]$^+$ + Cl$^-$ ⇌ [Ru^{II}(η^6-*p*-cymene)(L)(Cl)] + H$_2$O equilibria were studied for the bidentate (*O,O*) donor ligands **EHP** and **EHMP** using ^{1}H NMR spectroscopy. Spectra were recorded at pH 5.8 where the *mono*-ligand complexes predominate and at physiological pH (pH 7.4) using various chloride concentrations (Fig. S6). Fast ligand exchange processes were observed in the ^{1}H NMR spectra as the signals of the aqua and chlorido species do not appear separately: A shift of the location of the cymene-C*H* peaks by about 0.1 ppm was observed by elevating the chloride concentration. A similar tendency was seen at both pH values studied (Fig. 7). Based on these spectral changes the equilibrium constants for the water/chloride exchange reactions were estimated (Table 2). The calculations should be considered only as estimations since a high excess of chloride (~ 0.5 M) was necessary to obtain saturation curves for the Ru complexes with a chlorido rather than an aqua ligand and thus the ionic strength of the solutions was not constant at 0.2 M. This effect was reached at a somewhat lower chloride concentration in the case of **EHMP**, and consequently a slightly higher logK' value was obtained compared with **EHP**. According to these data about 38% and 55% of the **EHP** complex are chlorinated at 0.1 and 0.2 M chloride concentration, respectively, while for **EHMP** approximately 48% and 65% of the chlorinated species were found.

Fig. 7.

^{1}H NMR titrations of the [Ru^{II}(η^6-*p*-cymene)]$^{2+}$−ligand systems clearly revealed various overlapping processes above pH 6 (Fig. 5). When elevating the pH value, the *mono*-ligand complex starts to dissociate resulting in the trihydroxido-bridged dinuclear species and the free ligand, which features a pH-dependent signal as its proton dissociation falls in this pH range. The dissociation of the [Ru^{II}(η^6-*p*-cymene)(L)] species is relatively slow and could not be followed by pH-potentiometry as the real equilibria could not be reached during the time-

10

scale of this method (*max.* ~15 min at each point). This is a possible reason why the fit between the molar fractions calculated based on pH-potentiometry and ^{1}H NMR spectroscopic data at pH > 6.5 is not satisfactory. In addition, the hydrolysis products of the ester bond cleavage of the ligand, *i.e.*, the carboxylate and ethanol are also formed in solution at pH > ~9 (Fig. 5). Ester hydrolysis of the complexes occurs only at a slightly lower pH than for the ligands. Thus, no strong catalytic effect on the ligand hydrolysis of the metal ion is probable. According to this finding, the coordination *via* the carboxylate side chain after hydrolysis of the ester moiety is also not likely to occur at pH < 9. The hydrolytic stability of the $[Ru^{II}(\eta^6\text{-}p\text{-cymene})]^{2+}$–**EHP** ligand system was monitored at pH 7.40 by ^{1}H NMR spectroscopy for a week and only *ca.* 5% hydrolysis product was observed.

Besides the slow dissociation of the mono-ligand complex and the ester bond hydrolysis, a third process may be responsible for the significant shift of the ^{1}H NMR signals of the mono-ligand complex at pH > 8. Most probably the formation of a mixed hydroxido species $[Ru^{II}(\eta^6\text{-}p\text{-cymene})(L)(OH)]$ takes place. Due to the above mentioned slow complex dissociation processes, no reliable stability constant could be calculated for this complex based on pH-potentiometric experiments. However, pK_a values were estimated based on the pH-dependence of the signals of the C*H*(Ar) cymene protons in ^{1}H NMR spectra (Fig. S7, Table 2). The pK_a values of the *mono* complexes of **EHP** and **EHMP** are fairly similar and fall within the range found for half-sandwich Ru^{II} complexes with (*O,O*) coordinating ligands [9,14]. It is noteworthy that our data obtained in the presence of 0.2 M KCl are significantly higher as compared with the chloride-free medium [18], since the presence of competing chloride ions can suppress the hydrolysis of $[Ru^{II}(\eta^6\text{-}p\text{-cymene})(L)]$.

*3.4. Comparison of the stability of $[Ru^{II}(\eta^6\text{-}p\text{-cymene})]$ complexes of **EHP** with **EHMP** and other related ligands*

Direct comparison of the stability constants of the $[Ru^{II}(\eta^6\text{-}p\text{-cymene})]$ complexes formed with the ligands **EHP** and **EHMP** (Table 2) reveals that the presence of the extra methyl group on the aromatic ring results in higher $\log\beta$ values, although the pK_a of **EHMP** is also higher. Therefore, the overall stability constants of the $[Ru^{II}(\eta^6\text{-}p\text{-cymene})(L)]$ species were corrected by the different ligand basicities according to the following competition reaction:

$$[Ru^{II}(\eta^6\text{-}p\text{-cymene})] + HL \rightleftharpoons [Ru^{II}(\eta^6\text{-}p\text{-cymene})(L)] + H^+ \qquad (3)$$
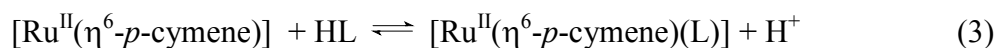
$$\log K^* = \log\beta\,[Ru^{II}(\eta^6\text{-}p\text{-cymene})(L)] - pK_a(HL) \qquad (4)$$

A higher log$K*$ implies more favored metal complex formation as compared with the protonated ligand. Based on these derived constants (log$K*$ in Table 2), the electron donating methyl group adjacent to the coordination site in **EHMP** slightly increases the metal binding ability. The 3,4-hydroxypyridone deferiprone and maltol as a 3-hydroxy-4-pyrone feature similar structures as **EHP** and **EHMP** and the stability of their mono-ligand Ru^{II}(arene) complexes, which predominate at physiological pH in the mM concentration range are higher with log$K*$ values of 2.08 and 0.61 reported for deferiprone and maltol, respectively [24]. Consequently, the stability order of the (*O,O*) chelates is the following: **EHP** < **EHMP** < maltol < deferiprone. These results fit the generally accepted stability trend, *i.e.*, 3-hydroxypyrid-4-ones > 3-hydroxypyrid-2-ones [35]. According to these results, it can be concluded that **EHP** and **EHMP** possess moderate binding ability towards [Ru^{II}(η^6-*p*-cymene)] and significant dissociation of their complexes or the displacement of the original carrier ligand by other bioligands are probable under biologically relevant conditions, namely at low concentrations and at pH 7.4.

4. Conclusions

The two alkoxycarbonylmethyl-3-hydroxy-2(1*H*)-pyridones **EHP** and **EHMP** feature ethyl ester groups, which were found to be stable against hydrolysis in the pH range 2.0−10.4 in aqueous solution. The methylated derivative **EHMP** has higher basicity and lipophilicity. The stoichiometry and stability of their Ru^{II}(η^6-*p*-cymene) complexes were determined by pH-potentiometry, ^{1}H NMR spectroscopy and UV-Vis spectrophotometry in aqueous solution. Formation of mono-ligand complexes was found with moderate stabilities in which the ligands coordinate in a bidentate fashion *via* their oxygen donors. These species predominate in the physiological pH range at mM concentrations, but considerable dissociation and the partial displacement of the original ligands by endogenous competitors is possible. In addition, chlorido/aqua co-ligand exchange processes for the [Ru^{II}(η^6-*p*-cymene)(L)(H$_2$O)]$^+$ species were monitored. Based on these data, it can be estimated that in the complex up to 55–65% of the aqua ligand is replaced by chlorido at 0.2 M chloride concentration. The ester groups of the ligands in [Ru^{II}(η^6-*p*-cymene)(L)(H$_2$O)]$^+$ show considerable hydrolysis only in the basic pH range where significant dissociation of the complex and formation of dinuclear

trihydroxido bridged $[Ru_2(\eta^6\text{-}p\text{-cymene})_2(OH)_3]$ and the hydroxido species $[Ru^{II}(\eta^6\text{-}p\text{-cymene})(L)(OH)]$ was found.

5. Abbreviations

CT	charge transfer
D	distribution coefficient
EHP	N-[(**e**thoxycarbonyl)methyl]-3-**h**ydroxy-2-(1*H*)-**p**yridone
EHMP	N-[(**e**thoxycarbonyl)methyl]-3-**h**ydroxy-4-**m**ethyl-2-(1*H*)-**p**yridone
MH2P	3-hydroxy-1-methylpyrid-2(1*H*)-one
P	partition coefficient

Acknowledgments

Appendix. Supplementary data

Supplementary data related to this article can be found online at…

References

[1] Y. Jung, S.J. Lippard, Chem. Rev. 107 (2007) 1387–1407.

[2] L.R. Bernstein, in: Metallotherapeutic Drugs and Metal-Based Diagnostic Agents: The Use of Metals in Medicine (Eds. M. Gielen, B.R.T. Tiekink) vol. 14, John Wiley & Sons, Ltd, 2005, pp. 259–277.

[3] M. Galanski, V.B. Arion, M.A. Jakupec, B.K. Keppler, Curr. Pharm. Des. 9 (2003) 2078–2089.

[4] P.J. Dyson, G. Sava, Dalton Trans. (2006) 1929–1933.

[5]   J.M. Rademaker-Lakhai, D. van den Bongard, D. Pluim, J.H. Beijnen, J.H. Schellens, Clin. Cancer Res. 10 (2004) 3717-3727.

[6]   E. Alessio, G. Mestroni, A. Bergamo, G. Sava, Current Topics in Med Chem 4 (2004) 1525–1535.

[7]   C.G. Hartinger, M.A. Jakupec, S. Zorbas-Seifried, M. Groessl, A. Egger, W. Berger, H. Zorbas, P.J. Dyson, B.K. Keppler, Chem. Biodiversity 5 (2008) 2140–2155.

[8]   C.G. Hartinger, S. Zorbas-Seifried, M.A. Jakupec, B. Kynast, H. Zorbas, B.K. Keppler, J. Inorg. Chem. 100 (2006) 891–904.

[9]   W. Kandioller, A. Kurzwernhart, M. Hanif, S.M. Meier, H. Henke, B.K. Keppler, C.G. Hartinger; J. Organomet. Chem. 696 (2011) 999−1010.

[10]   W. Kandioller, C.G. Hartinger, A.A. Nazarov, C. Bartel, M. Skocic, M.A. Jakupec, V.B. Arion, B.K. Keppler, Chem. Eur. J. 15 (2009) 12283–12291.

[11]   J. Kljun, A.K. Bytzek, W. Kandioller, C. Bartel, M.A. Jakupec, C.G. Hartinger, B.K. Keppler, I. Turel, Organometallics 30 (2011) 2506–2512.

[12]   N. Gligorijević, S. Aranđelović, L. Filipović, K. Jakovljević, R. Janković, S. Grgurić-Šipka, I. Ivanović, S. Radulović, Ž. Lj. Tešić, , J. Inorg. Biochem. 108 (2012) 53–61.

[13]   W.H. Ang, A. Casini, G. Sava, P.J. Dyson, J. Organomet. Chem. 696 (2011) 989–998.

[14]   A.M. Pizarro, M. Melchart, A. Habtemariam, L. Salassa, F.P.A. Fabbiani, S. Parsons, P.J. Sadler, Inorg. Chem. 49 (2010) 3310–3319.

[15]   F. Wang, H. Chen, S. Parsons, I.D.H. Oswald, J.E. Davidson, P.J. Sadler, Chem. Eur. J. 9 (2003) 5810–5820.

[16]   F. Beckford, J. Thessing, J. Woods, J. Didion, N. Gerasimchuk, A. Gonzalez-Sarrias, N.P. Seeram, Metallomics 3 (2011) 491–502.

[17]   M. Hanif, S.M. Meier, W. Kandioller, A. Bytzek, M. Hejl, C.G. Hartinger, A. A. Nazarov, V.B. Arion, M.A. Jakupec, P.J. Dyson, B.K. Keppler, J. Inorg. Biochem. 105 (2011) 224–231.

[18]   M. Hanif, H. Henke, S.M. Meier, S.Martic, M. Labib, W. Kandioller, A. Jakupec, V.B. Arion, H.B. Kraatz, B.K. Keppler, C.G. Hartinger, Inorg. Chem. 49 (2010) 7953–7963.

[19]   M. Hanif, A.A. Nazarov, C.G. Hartinger, W. Kandioller, M.A. Jakupec, V.B. Arion, P.J. Dyson, B.K. Keppler, Dalton Trans. 39 (2010) 7345–7352.

[20]   F. Wang, H. Chen, S. Parsons, I.D.H. Oswald, J.E. Davidson, P.J. Sadler, Chem. Eur. J. 9 (2003) 5810–5820.

[21]   A.F.A. Peacock, P.J. Sadler, Chem. Asian J. 3 (2008) 1890–1899.

[22]   C.G. Hartinger, P.J. Dyson, Chem. Soc. Rev. 38 (2009) 391–401.

[23]   P. Buglyó, E. Farkas, Dalton Trans. 39 (2009) 8063−8070.

[24]   L. Bíró, E. Farkas, P. Buglyó, Dalton Trans. 39 (2010) 10272−10278.

[25]   R. Fernandez, M. Melchart, A. Habtemariam, S. Parsons, P.J. Sadler, Chem. Eur. J. 10 (2004) 5173–5179.

[26]   W. Kandioller, C.G. Hartinger, A.A. Nazarov, M.L. Kuznetsov, R.O. John, C. Bartel, M.A. Jakupec, V.B. Arion, B.K. Keppler, Organometallics 28 (2009) 4249–4251

[27]   E.A. Enyedy, E. Sija, T. Kiss, C.G. Hartinger, B.K. Keppler, T. Jakusch, *unpublished data*

[28]   G. Gran, Acta Chem. Scand. 4 (1950) 559−577.

[29]   M.A. Bennett, T.N. Huang, T.W. Matheson, A.K. Smith, Inorg. Synth. 21 (1982) 74–78.

[30]   H.M. Irving, M.G. Miles, L.D. Pettit, Anal. Chim. Acta 38 (1967) 475–488.

[31]   SCQuery, The IUPAC Stability Constants Database, Academic Software (Version 5.5), Royal Society of Chemistry, 1993–2005.

[32]   P. Gans, A. Sabatini, A. Vacca, Talanta 43 (1996) 1739−1753.

[33]   L. Zékány, I. Nagypál, in: Computational Methods for the Determination of Stability Constants (Ed.: D. L. Leggett), Plenum Press, New York, 1985, pp. 291−353.

[34]   S.K. Poole, C.F. Poole, J. Chromatogr. B 797 (2003) 3−19.

[35]   E.T. Clarke, A.E. Martell, Inorg. Chim. Acta 196 (1992) 185−194.

[36]   L. Bíró, E. Farkas, P. Buglyó, Dalton Trans. 41 (2012) 285−291.

[37]   L. Carter, D.L. Davies, J. Fawcett, D.R. Russel, Polyhedron 12 (1993) 1599−1602.

[38]   A.F.A. Peacock, M. Melchart, R.J. Deeth, A. Habtemariam, S. Parsons, P.J. Sadler, Chem. Eur. J. 13 (2007) 2601 – 2613.

[39]   A.J. Godó, A.Cs. Bényei, B. Duff, D.A. Egan, P. Buglyó, RSC Advances 2 (2012) 1486−1495.

Table 1

Proton dissociation constants (pK_a) of **EHP** and **EHMP** with λ_{max}, molar absorptivity (M^{-1}cm^{-1}) and calculated chemical shift (ppm) values for ligand species determined by UV spectrophotometric and ^{1}H NMR titrations (T = 25.0 °C, I = 0.20 M (KCl)).[a]

	EHP		**EHMP**	
pK_a (pH-potentiometry)	8.60(2)		9.20(3)	
pK_a (UV)	8.58(1)		9.21(1)	
pK_a (^{1}H NMR)	8.56(1)		9.19(1)	
log$D_{7.4}$	−0.10(1)		+0.64(2)	
log$P$	−0.07		+0.65	
	HL	**L$^-$**	**HL**	**L$^-$**
λ_{max} (nm) /	300 / 6156	314 / 7485	298 / 6881	312 / 8718
ε (mol^{-1}dm^{3}cm^{-1})	238 / 3227	260 / 4935	242 / 2616	267 / 5427
δ / ppm[b]	**HL**	**L$^-$**	**HL**	**L$^-$**
CH(4) (d)	7.179	6.767	−	−
CH_3(4) (s)	−	−	2.187	2.087
CH(5)[c]	6.440	6.313	7.112	6.725
CH(6) (d)	7.086	6.562	6.403	6.316
CH_2 (q)[d]	4.264	4.250	4.256	4.242
CH_3 (t)[d]	1.271	1.271	1.266	1.266

[a] Uncertainties (SD) are shown in parentheses for the species characterized in the present work.
[b] The signal of -CH_2C=O (s) lies underneath the water peak.
[c] CH(5) **EHP**: (d/d), **EHMP**: (d)
[d] Data of ethanol for comparison: CH_2 (q) = 3.65 ppm; CH_3 (t) = 1.17 ppm

Table 2

Overall stability constants ($\log\beta$) with some stepwise and derived constants of the [Ru^{II}(η^6-*p*-cymene)] complexes of **EHP** and **EHMP** ($T = 25.0$ °C, $I = 0.20$ M (KCl))[a]

	EHP	EHMP
$\log\beta$ ([Ru^{II}(η^6-*p*-cymene)(L)]) (pH-metry)	8.49(1)	9.33(1)
$\log\beta$ ([Ru^{II}(η^6-*p*-cymene)(L)]) (UV−Vis)	8.55(9)	9.30(1)
pK_a ([Ru^{II}(η^6-*p*-cymene)(L)]) (^{1}H NMR)[b]	9.39(1)	9.46(3)
logK' (H$_2$O/Cl$^-$)[c]	0.78(2)	0.96(2)
log$K*$ [d]	−0.11	+0.13

[a] Uncertainties (SD) are shown in parentheses for the species characterized in the present work. Hydrolysis products of the metal ion: $\log\beta$ [Ru$_2$(η^6-*p*-cymene)$_2$H$_{-2}$]$^{2+}$ = −7.01(1) and $\log\beta$ [(Ru$_2$(η^6-*p*-cymene)$_2$H$_{-3}$]$^+$ = −11.99(1).
[b] [Ru^{II}(η^6-*p*-cymene)(L)] $\rightleftharpoons$ [Ru^{II}(η^6-*p*-cymene)(L)(OH)] + H$^+$
[c] [Ru^{II}(η^6-*p*-cymene)(L)(H$_2$O)]$^+$ + Cl$^-$ $\rightleftharpoons$ [Ru^{II}(η^6-*p*-cymene)(L)(Cl)] + H$_2$O
[d] log$K*$ = $\log\beta$ [Ru^{II}(η^6-*p*-cymene)(L)] – pK_a(HL)
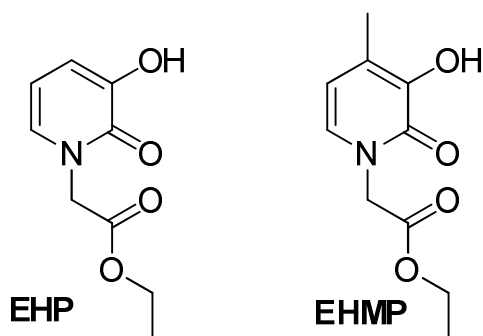
Chart 1. Ligands used in this study: **EHP** = *N*-[(**e**thoxycarbonyl)methyl]-3-**h**ydroxy-2-(1*H*)-**p**yridone; **EHMP** = *N*-[(**e**thoxycarbonyl)methyl]-3-**h**ydroxy-4-**m**ethyl-2-(1*H*)-**p**yridone
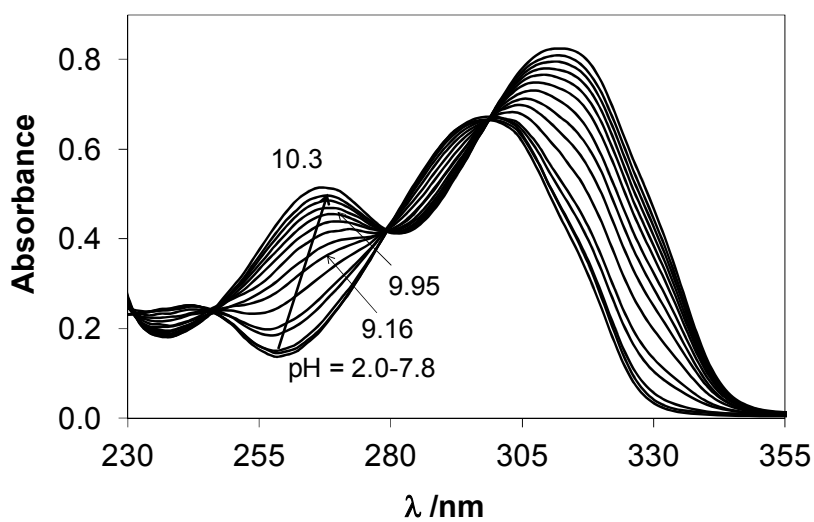

Fig. 1. UV absorbance spectra of ligand **EHMP** recorded in the pH range of 2.0−10.3 (c_{EHP} = 0.1 mM; T = 25.0 °C; I = 0.20 M (KCl)).
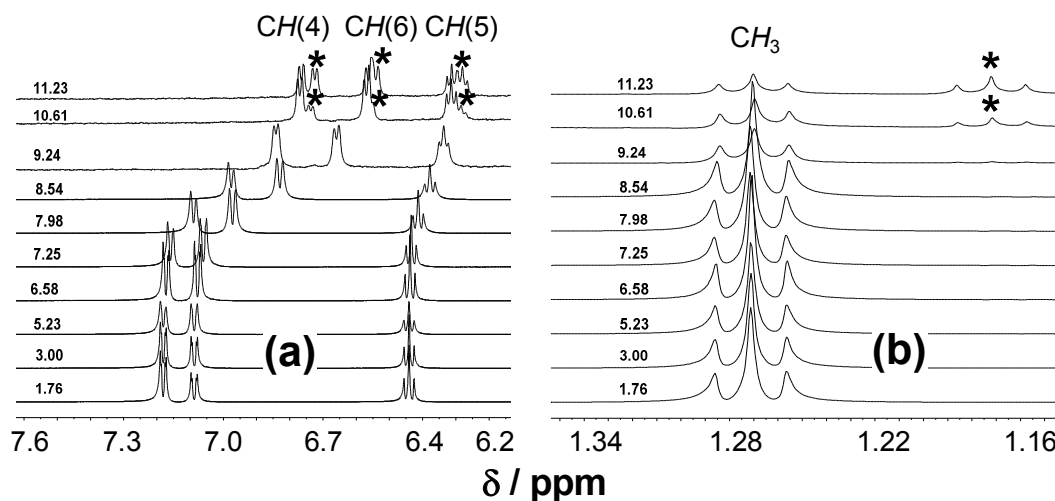
Fig. 2. Low (a) and high (b) field regions of the ^{1}H NMR spectra of **EHP** recorded at the indicated pH values ($c_{\textbf{EHP}}$ = 4 mM; T = 25.0 °C; I = 0.20 M (KCl); 10% D_2O). The peaks stemming from the hydrolysis products 3-hydroxy-2-oxopyridine-1(2H)-carboxylate (on a) and ethanol (on b) are annotated with stars.
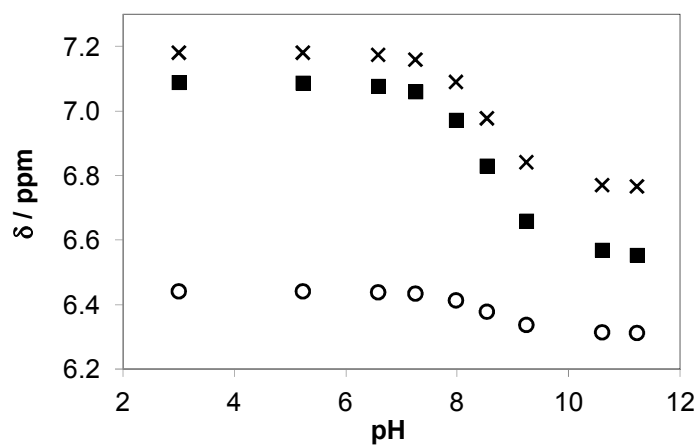
Fig. 3. pH-Dependence of the chemical shifts (δ) of the **EHP** protons: CH(4) (×); CH(6) (■); CH(5) (○) (T = 25.0 °C; I = 0.20 M (KCl); 10% D_2O).
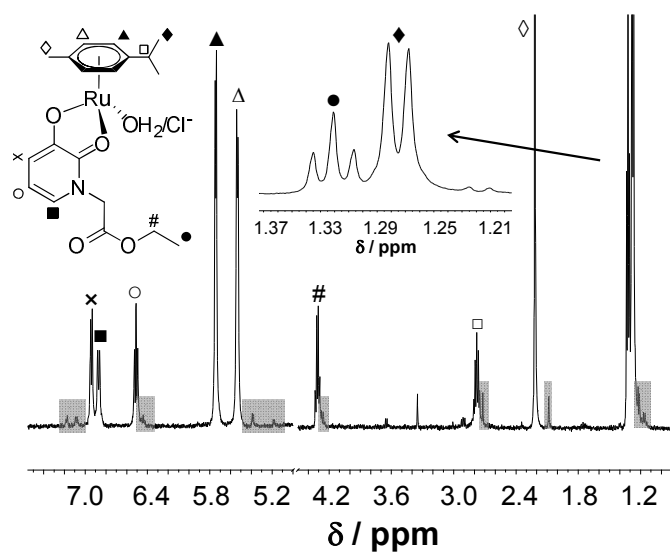
Fig. 4. ^{1}H NMR spectrum of the [Ru^{II}(η^6-*p*-cymene)]–**EHP** system recorded at pH 6.09. The peaks with the grey background correspond to non-bound ligand and metal ion (c_{EHP} = 2 mM; M:L = 1:1; T = 25.0 °C, I = 0.20 M (KCl), 10% D$_2$O).
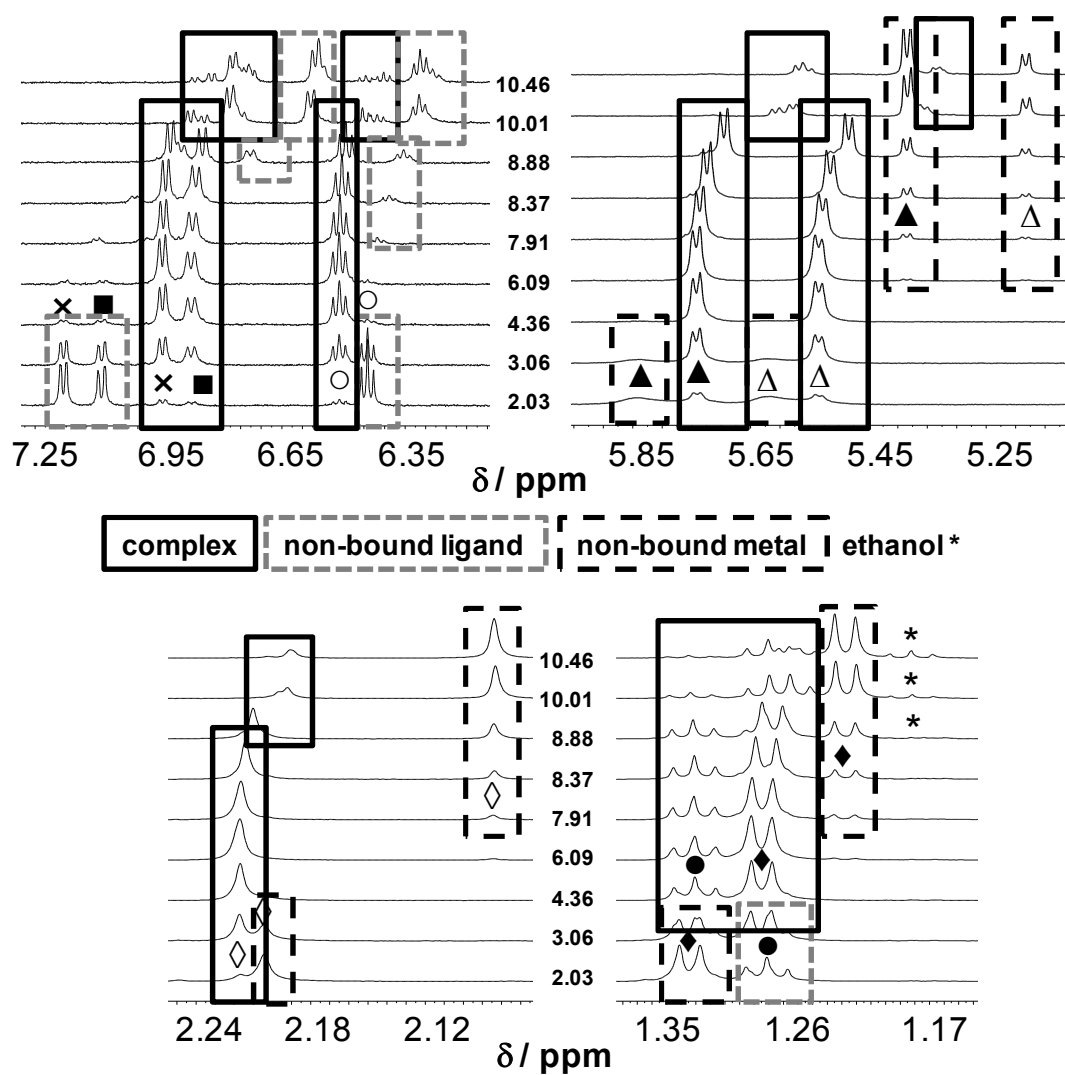
Fig. 5. Representative ^{1}H NMR spectra of the $[Ru^{II}(\eta^6\text{-}p\text{-cymene})]$–**EHP** system recorded at various pH values (c_{EHP} = 2 mM; M:L = 1:1; T = 25.0 °C, I = 0.20 M (KCl), 10% D_2O).
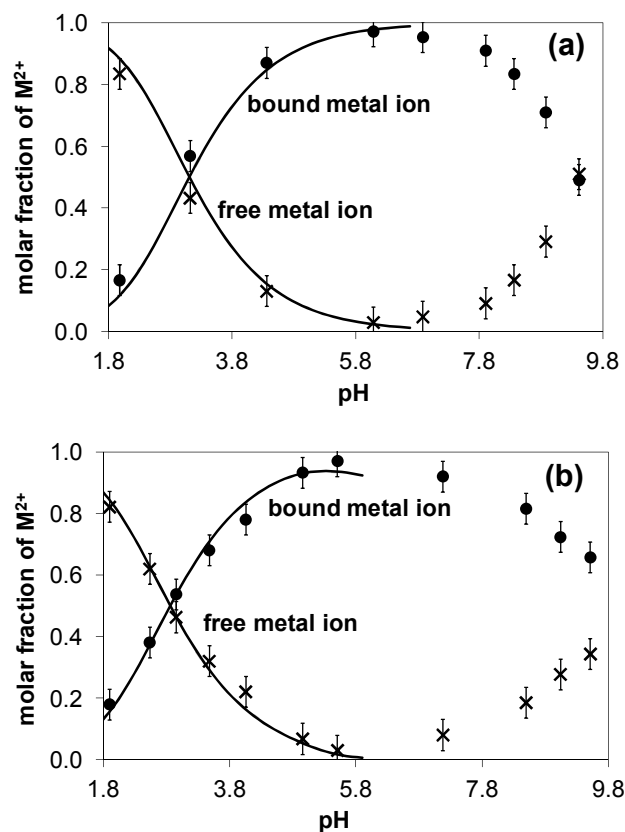
Fig. 6. Bound and ligand-free metal ion fractions for the [Ru^{II}(η^6-p-cymene)]–**EHP** (a) and – **EHMP** (b) systems calculated on the basis of the stability constants of the [Ru^{II}(η^6-p-cymene)(L)] species (solid lines) and ^{1}H NMR peak integrals of the singlet CH_3 (cymene moiety) protons: bound (●), free (×) fractions. Errors are calculated with the help of the ligand distribution on basis of the ligand peaks in the NMR spectra (c_{ligand} = 2 mM; M:L = 1:1; T = 25.0 °C, I = 0.20 M (KCl), 10% D$_2$O).
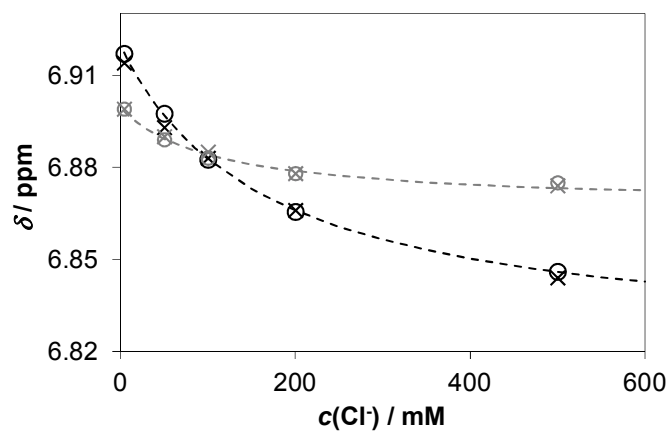
Fig. 7. ^{1}H NMR chemical shifts (δ) of the CH(6) and CH(5) peaks of the [Ru^{II}(η^6-p-cymene)(L)]$^+$ complexes of **EHP** (black) and **EHMP** (grey), respectively, plotted against the chloride concentration at pH 5.8 ($\circ$) and 7.4 ($\times$) together with the fitted curves ($c_{ligand} = 2$ mM; M:L = 1:1; $T = 25.0$ °C, 10% D$_2$O).